

A fast vector penalty-projection method for incompressible non-homogeneous or multiphase Navier-Stokes problems

Philippe Angot^a, Jean-Paul Caltagirone^b, and Pierre Fabrie^c

^aAix-Marseille Université, LATP - Centre de Mathématiques et Informatique, CNRS UMR7353, 13453 Marseille Cedex 13 - France.

^bUniversité de Bordeaux & IPB, Institut de Mécanique et d'Ingénierie de Bordeaux, CNRS UMR5295, 33400 Talence - France.

^cUniversité de Bordeaux & IPB, Institut Mathématiques de Bordeaux CNRS UMR5251, ENSEIRB-MATMECA, Talence - France.

Abstract

We present a new *fast vector penalty-projection method* (VPP_ε) to efficiently compute the solution of unsteady Navier-Stokes problems governing incompressible multiphase viscous flows with variable density and/or viscosity. The key idea of the method is to compute at each time step an accurate and curl-free approximation of the pressure gradient increment in time. This method performs a *two-step approximate divergence-free vector projection* yielding a velocity divergence vanishing as $O(\varepsilon \delta t)$, δt being the time step, with a penalty parameter ε as small as desired until the machine precision, e.g. $\varepsilon = 10^{-14}$, whereas the solution algorithm can be extremely fast and cheap. Indeed, the proposed *vector correction step* typically requires only a few iterations of a suitable preconditioned Krylov solver whatever the spatial mesh step. The method is numerically validated on three benchmark problems for non-homogeneous or multiphase flows where we compare it to the Uzawa augmented Lagrangian (UAL) and scalar incremental projection (SIP) methods. Moreover, a new test case for fluid-structure interaction problems is also investigated. That results in a very robust method running faster than usual methods and being able to efficiently and accurately compute sharp test cases whatever the density, viscosity or anisotropic permeability jumps, whereas other methods crash.

Keywords: Vector penalty-projection method, Divergence-free penalty-projection, Penalty method, Splitting prediction-correction scheme, Navier-Stokes equations, incompressible non-homogeneous or multiphase flows.

2010 MSC: 35Q30, 35Q35, 49M30, 65M08, 65M85, 65N08, 65N85, 74F10, 76D05, 76D45, 76M12, 76R10, 76T10

1. Introduction on the models for non-homogeneous or multiphase flows

Let $\Omega \subset \mathbb{R}^d$ ($d = 2$ or 3 in practice) be an open bounded and connected domain with a Lipschitz continuous boundary $\Gamma = \partial\Omega$ and \mathbf{n} be the outward unit normal vector on Γ .

For $T > 0$, we consider the following unsteady Navier-Stokes/Brinkman problem [1, 3, 19] governing incompressible non-homogeneous or multiphase flows where Dirichlet boundary conditions for the velocity $\mathbf{v}|_\Gamma = 0$ on Γ , the volumic force \mathbf{f} and initial data $\mathbf{v}(t = 0) = \mathbf{v}_0$, $\varphi(t = 0) = \varphi_0 \in L^\infty(\Omega)$ with $\varphi_0 \geq 0$ a.e. in Ω , are given. For sake of brevity here, we just focus on the model problem (1-3) where $\mathbf{d}(\mathbf{v}) = (\nabla \mathbf{v} + (\nabla \mathbf{v})^T)/2$, as a part of more complex fluid mechanics problems.

$$\rho(\partial_t \mathbf{v} + (\mathbf{v} \cdot \nabla) \mathbf{v}) - 2 \nabla \cdot (\mu \mathbf{d}(\mathbf{v})) + \mu \mathbf{K}^{-1} \mathbf{v} + \nabla p = \mathbf{f} \quad \text{in } \Omega \times (0, T) \quad (1)$$

$$\nabla \cdot \mathbf{v} = 0 \quad \text{in } \Omega \times (0, T) \quad (2)$$

$$\partial_t \varphi + \mathbf{v} \cdot \nabla \varphi = 0 \quad \text{in } \Omega \times (0, T). \quad (3)$$

Email addresses: angot@cmi.univ-mrs.fr (Philippe Angot), calta@enscbp.fr (Jean-Paul Caltagirone), pierre.fabrie@math.u-bordeaux1.fr (and Pierre Fabrie)

URL: <http://www.latp.univ-mrs.fr/~angot> (Philippe Angot)

The permeability tensor \mathbf{K} in the Darcy term is supposed to be symmetric, uniformly positive definite and bounded in Ω . The equation (3) for the phase function φ governs the transport by the flow of the interface between two phases, either fluid or solid, respectively in the case of two-phase fluid flows or fluid-structure interaction problems. The force \mathbf{f} may include some volumic forces like the gravity force $\rho \mathbf{g}$ as well as the surface tension force to describe the capillarity effects at the phase interfaces Σ . The advection-diffusion equation for the temperature \mathcal{T} is not precised here and we assume some given state laws: $\mu = \mu(\varphi, \mathcal{T})$ and $\rho = \rho(\varphi, \mathcal{T})$ for each phase, where the functions are continuous and positive. The case of nonhomogeneous velocity Dirichlet boundary conditions, $\mathbf{v}|_{\Gamma} = \mathbf{v}_D$ on Γ , also requires some given boundary conditions for φ on the inflow part Γ^- of Γ where $\mathbf{v}_D \cdot \mathbf{n}|_{\Gamma} < 0$.

2. The fast vector-penalty projection method (VPP _{ε})

We describe hereafter the two-step vector penalty-projection (VPP _{ε}) method with a penalty parameter $0 < \varepsilon \ll 1$. It is issued from noticeable improvements of previous works [12, 5, 7] or from [17, 18, 9, 14] using the augmented Lagrangian splitting introduced in [7]. The method is briefly introduced in [6] with some preliminary results. The convergence of the continuous artificial compressibility version of the basic (VPP _{r, ε}) method proposed in [5, 7] is proved in [8] for the homogeneous Navier-Stokes equations.

For ρ^0, φ^0, μ^0 with $\rho^0, \varphi^0 \geq 0, \mu^0 > 0$ a.e. in Ω , \mathbf{v}^0 and p^0 given, the method reads as below with usual notations for the semi-discrete setting in time, $\delta t > 0$ being the time step. For all $n \in \mathbb{N}$ such that $(n+1)\delta t \leq T$, find $\mathbf{v}^{n+1}, p^{n+1}, \varphi^{n+1}$ and then $\rho^{n+1} = \rho(\varphi^{n+1}), \mu^{n+1} = \mu(\varphi^{n+1})$ such that:

$$\rho^n \left(\frac{\tilde{\mathbf{v}}^{n+1} - \mathbf{v}^n}{\delta t} + (\mathbf{v}^n \cdot \nabla) \tilde{\mathbf{v}}^{n+1} \right) - 2 \nabla \cdot (\mu^n \mathbf{d}(\tilde{\mathbf{v}}^{n+1})) + \mu^n \mathbf{K}^{-1} \tilde{\mathbf{v}}^{n+1} + \nabla p^n = \mathbf{f}^n \quad \text{in } \Omega \quad (4)$$

$$\varepsilon \left(\frac{\rho^n}{\delta t} \mathbf{I} + \mu^n \mathbf{K}^{-1} \right) \hat{\mathbf{v}}^{n+1} - \nabla (\nabla \cdot \hat{\mathbf{v}}^{n+1}) = \nabla (\nabla \cdot \tilde{\mathbf{v}}^{n+1}) \quad \text{in } \Omega \quad (5)$$

$$\mathbf{v}^{n+1} = \tilde{\mathbf{v}}^{n+1} + \hat{\mathbf{v}}^{n+1}, \quad \text{and} \quad \nabla(p^{n+1} - p^n) = - \left(\frac{\rho^n}{\delta t} \mathbf{I} + \mu^n \mathbf{K}^{-1} \right) \hat{\mathbf{v}}^{n+1} \quad \text{in } \Omega \quad (6)$$

$$p^{n+1} = p^n + \phi^{n+1} \quad \text{with } \phi^{n+1} \text{ reconstructed from its gradient} \quad \nabla \phi^{n+1} = - \left(\frac{\rho^n}{\delta t} \mathbf{I} + \mu^n \mathbf{K}^{-1} \right) \hat{\mathbf{v}}^{n+1} \quad \text{in } \Omega \quad (7)$$

$$\frac{\varphi^{n+1} - \varphi^n}{\delta t} + \mathbf{v}^{n+1} \cdot \nabla \varphi^n = 0 \quad \text{in } \Omega \quad (8)$$

with: $\tilde{\mathbf{v}}|_{\Gamma}^{n+1} = 0$, or for non homogeneous Dirichlet conditions: $\tilde{\mathbf{v}}|_{\Gamma}^{n+1} = \mathbf{v}_D^{n+1}$, and $\hat{\mathbf{v}}^{n+1} \cdot \mathbf{n}|_{\Gamma} = 0$. Here \mathbf{v}^n, p^n are desired to be first-order approximations of the exact velocity and pressure solutions $\mathbf{v}(t_n), p(t_n)$ at time $t_n = n \delta t$.

The consistency of the (VPP _{ε}) method is ensured with (6) since we have:

$$\rho^n \frac{\mathbf{v}^{n+1} - \tilde{\mathbf{v}}^{n+1}}{\delta t} + \mu^n \mathbf{K}^{-1} (\mathbf{v}^{n+1} - \tilde{\mathbf{v}}^{n+1}) + \nabla(p^{n+1} - p^n) = 0 \quad \text{with} \quad \mathbf{v}^{n+1} - \tilde{\mathbf{v}}^{n+1} = \hat{\mathbf{v}}^{n+1}, \quad (9)$$

which yields the effective problem solved with this method by summing with Eq. (4). The key feature of our method is to calculate an accurate and curl-free approximation of the momentum vector correction $\rho^n \hat{\mathbf{v}}^{n+1}$ in (5), at least when there is no Darcy term. Indeed (5-6) ensures that $(\rho^n / \delta t \mathbf{I} + \mu^n \mathbf{K}^{-1}) \hat{\mathbf{v}}^{n+1}$ is exactly a gradient which justifies the choice for $\nabla \phi^{n+1} = \nabla(p^{n+1} - p^n)$ since we have:

$$\left(\frac{\rho^n}{\delta t} \mathbf{I} + \mu^n \mathbf{K}^{-1} \right) \hat{\mathbf{v}}^{n+1} = \frac{1}{\varepsilon} \nabla (\nabla \cdot \mathbf{v}^{n+1}) \quad \Rightarrow \quad \nabla(p^{n+1} - p^n) = - \left(\frac{\rho^n}{\delta t} \mathbf{I} + \mu^n \mathbf{K}^{-1} \right) \hat{\mathbf{v}}^{n+1} = - \frac{1}{\varepsilon} \nabla (\nabla \cdot \mathbf{v}^{n+1}). \quad (10)$$

The (VPP _{ε}) method really takes advantage of the splitting method proposed in [6] for augmented Lagrangian systems or general saddle-point computations to get a very fast solution of (5); see Theorem 3.1. When we need the pressure field itself, e.g. to compute stress vectors, it is calculated in an incremental way as an auxiliary step. We propose to reconstruct $\phi^{n+1} = p^{n+1} - p^n$ from its gradient $\nabla \phi^{n+1}$ given in (6) with the following method.

Reconstruction of $\phi^{n+1} = p^{n+1} - p^n$ from its gradient.

By circulating on a suitable path starting at a point on the border where $\phi^{n+1} = 0$ is fixed and going through all

the pressure nodes in the mesh, we get with the gradient formula between two neighbour points A and B using the mid-point quadrature:

$$\phi^{n+1}(B) - \phi^{n+1}(A) = \int_A^B \nabla \phi^{n+1} \cdot d\mathbf{l} = - \int_A^B \frac{\rho^n}{\delta t} \hat{\mathbf{v}}^{n+1} \cdot d\mathbf{l} \approx - \frac{\rho^n}{\delta t} |\hat{\mathbf{v}}^{n+1}| h_{AB} \quad \text{with } h_{AB} = \text{distance}(A, B). \quad (11)$$

The field ϕ^{n+1} is calculated point by point from the boundary and then passing successively by all the pressure nodes. This fast algorithm is performed at each time step to get the pressure field p^{n+1} from the known field p^n .

3. On the fast discrete solution to the (VPP _{ε}) method

The great interest to solve (5) instead of a usual augmented Lagrangian problem lies in the following result issued from [7] which shows that the method can be ultra-fast and very cheap if $\eta = \varepsilon/\delta t$ is sufficiently small.

Let us now consider any space discretization of our problem in the case with no Darcy term for sake of shortness. We denote by $B = -\text{div}_h$ the $m \times n$ matrix corresponding to the discrete divergence operator, $B^T = \text{grad}_h$ the $n \times m$ matrix corresponding to the discrete gradient operator, whereas I denotes the $n \times n$ identity matrix with $n > m$ and D the $n \times n$ diagonal nonsingular matrix containing all the discrete density values of $\rho^n > 0$ a.e. in Ω . Here n is the number of velocity unknowns whereas m is the number of pressure unknowns. Then, the discrete vector penalty-projection problem corresponding to (5) with $\varepsilon = \eta \delta t$ reads:

$$\left(D + \frac{1}{\eta} B^T B \right) \hat{\mathbf{v}}_\eta = - \frac{1}{\eta} B^T B \tilde{\mathbf{v}}, \quad \text{with } \mathbf{v}_\eta = \tilde{\mathbf{v}} + \hat{\mathbf{v}}_\eta. \quad (12)$$

We proved in [7] the crucial result below due to the *adapted right-hand side* in the correction step (12) which lies in the range of the limit operator $B^T B$. Indeed, (12) can be viewed as a singular perturbation problem with well-suited data in the right-hand side. More precisely, we give in Theorem 3.1 the asymptotic expansion of the solution $\hat{\mathbf{v}}_\eta$ to (12):

$$\hat{\mathbf{v}}_\eta = - \frac{1}{\eta} \left(D + \frac{1}{\eta} B^T B \right)^{-1} B^T B \tilde{\mathbf{v}} \quad (13)$$

when the penalty parameter η is chosen sufficiently small; see the proof in [7, Theorem 1.1 and Corollary 1.3].

Theorem 3.1 (Fast solution of the discrete vector penalty-projection). *Let D be an $n \times n$ positive definite diagonal matrix, I the $n \times n$ identity matrix and B an $m \times n$ matrix. If the rows of B are linearly independent, $\text{rank}(B) = m$, then for all η small enough, $0 < \eta < 1/\|S^{-1}\|$ where $S = BD^{-1}B^T$, there exists an $n \times n$ matrix C_1 bounded independently on η such that the solution of the correction step (13) writes for any vector $\tilde{\mathbf{v}} \in \mathbb{R}^n$:*

$$\hat{\mathbf{v}}_\eta = C_0 \tilde{\mathbf{v}} + \eta C_1 \tilde{\mathbf{v}} \quad \text{with} \quad C_0 = -D^{-1} B^T (BD^{-1} B^T)^{-1} B, \quad C_1 = D^{-1} B^T S^{-2} \sum_{k=0}^{\infty} (-1)^k \eta^k S^{-k} B. \quad (14)$$

If $\text{rank}(B) = p < m$, there exists a surjective $p \times n$ matrix T such that $B^T B = T^T T$ and the similar result holds replacing B by T .

Hence, for a constant density $\rho > 0$ and choosing now $\eta = \rho \varepsilon / \delta t$, we have: $D = I$, $S = BB^T$ and $C_0 = -B^T S^{-1} B = -B^T (BB^T)^{-1} B$. Moreover, if $\text{rank}(B) = p \leq m \leq n$, the zero-order solution $\hat{\mathbf{v}} = C_0 \tilde{\mathbf{v}}$ in (14) is the solution of minimal Euclidean norm in \mathbb{R}^n to the linear system: $B \hat{\mathbf{v}} = -B \tilde{\mathbf{v}}$ by the least-squares method, and the matrix $B^\dagger = B^T (BB^T)^{-1}$ is the Moore-Penrose pseudo-inverse of B such that $C_0 = -B^\dagger B$. Indeed, a singular value decomposition (SVD) or a QR factorization of B yields: $C_0 = -I_0$ where I_0 is the $n \times n$ diagonal matrix having only 1 or 0 coefficients, the zero entries in the diagonal being the $n - p$ null eigenvalues of the operator $B^T B$.

Hence, for η small enough, the computational effort required to solve (12) amounts to approximate the matrix C_0 which includes both D and D^{-1} inside non commutative products. Thus, we always use the diagonal preconditioning in the case of a variable density which makes the effective condition number quasi-independent of the density jumps. We also use the Jacobi preconditioner in the prediction step (4) to cope with the viscosity or permeability jumps as performed in [19]. However, for a constant density when $D = I$, we get $C_0 = -I_0$. This explains why the solution can be obtained with only one iteration of a suitable preconditioned conjugate gradient whatever the size of the mesh step or the dimension n ; see the numerical results in [7] and Figure 3.

4. Numerical validations with discrete operator calculus methods

The (VPP_ε) method has been implemented with discrete exterior calculus (DEC) methods, see the recent review in [10], for the space discretization of the Navier-Stokes equations on unstructured staggered meshes. The (DEC) methods ensure primary and secondary discrete conservation properties. In particular, the space discretization satisfies for the discrete operators: $\nabla_h \times (\nabla_h \phi) = 0$ and $\nabla_h \cdot (\nabla_h \times \psi) = 0$, as for the structured MAC grid, which is not usually verified by other methods; see [10]. So, the (VPP_ε) method is validated on unstructured meshes both in 2-D or 3-D.

The structure and solver of the computational code are issued from previous works, originally implemented with a Navier-Stokes finite volumes solver on the staggered MAC mesh and using the Uzawa augmented Lagrangian (UAL) method to deal with the divergence-free constraint; see [13, 19]. We refer to [4, 1, 3, 19] and the references therein for the analysis and numerical validations of the fictitious domain model using the so-called L^2 or H^1 -volume penalty methods to take account of obstacles in flow problems with the Navier-Stokes/Brinkman equations. Hence, our approach is essentially Eulerian with a Lagrangian front-tracking of the sharp interfaces accurately reconstructed on the fixed Eulerian mesh, see e.g. [19, 22, 23] and the references therein. Thus we use no Arbitrary Lagrangian-Eulerian (ALE) method, no global remeshing nor moving mesh method. The augmented Lagrangian method has been improved by using an adaptive augmentation parameter, e.g. [23], to get a more robust (UAL) method. This allows us to consider the solutions obtained by the (UAL) method as reference solutions since the augmented Lagrangian method does not suffer from splitting errors. Moreover, a scalar incremental projection (SIP) method [15] has been also implemented within the same computational code in order to compare the numerical results. All the linear algebraic systems for the three methods, e.g. the prediction steps, are solved with the Krylov *BiCGStab2* algorithm preconditioned by the incomplete *LU* factorization of order zero *ILU(0)*.

4.1. Homogeneous flows: Green-Taylor vortex analytical solution

The first test case is the unsteady Green-Taylor vortex such that the mean steady velocity field is of order $V_0 = 1$. The analytical solution in the square domain $\Omega =]-0.5, 0.5]^2$ reads as follows with $\rho = 1$ and μ given by $1/\text{Re}$:

$$\begin{cases} u(x, y, t) = -V_0 \cos(\pi x) \sin(\pi y) (1 - \exp(-\pi V_0 t)), & v(x, y, t) = V_0 \sin(\pi x) \cos(\pi y) (1 - \exp(-\pi V_0 t)) \\ p(x, y, t) = -\frac{\rho V_0^2}{2} (\cos^2(\pi x) + \cos^2(\pi y)) (1 - \exp(-\pi V_0 t))^2 \\ S_u(x, y, t) = -2\pi^2 \mu V_0 \cos(\pi x) \sin(\pi y) (1 - \exp(-\pi V_0 t)) + \rho \partial_t u \\ S_v(x, y, t) = 2\pi^2 \mu V_0 \sin(\pi x) \cos(\pi y) (1 - \exp(-\pi V_0 t)) + \rho \partial_t v. \end{cases}$$

The scheme is $O(\delta t)$ accurate in time for the velocity, pressure and pressure gradient, see Figure 1 (left), whereas it is $O(h^2)$ accurate in space, see Figure 1 (right). We also observe in Figure 2 (left) that the L^2 -norm of the velocity divergence vanishes as $O(\varepsilon \delta t)$, like for the $(VPP_{r,\varepsilon})$ method proposed in [5, 7].

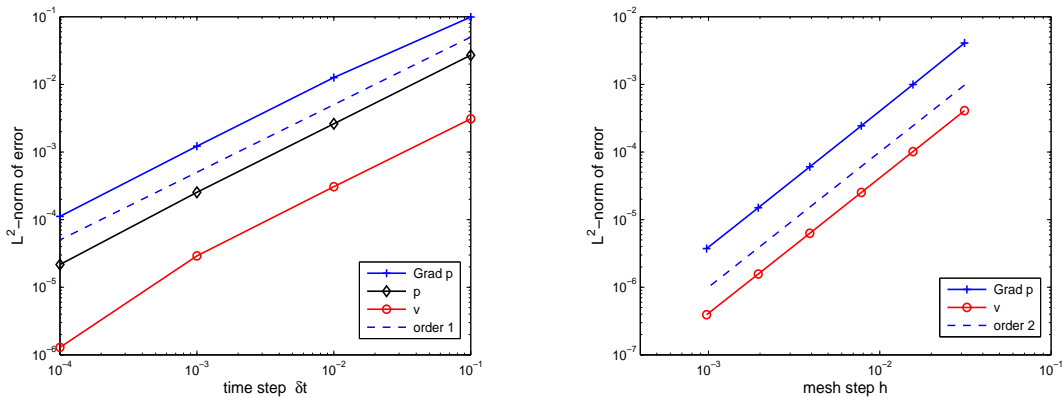


Figure 1: (VPP_ε) method with $\varepsilon = 10^{-4}$ for the Green-Taylor vortex at $\text{Re} = 1$ - LEFT: Time convergence with time step δt at $t = 0.1$ for the unsteady vortex with $h = 1/128$, $\|res\|_2 \leq 10^{-10}$. RIGHT: Space convergence with mesh size h for the steady vortex.

4.2. Dilatable flows: Rayleigh-Bénard thermal convection

The second benchmark problem is the Rayleigh-Bénard thermal natural convection inside a square differentially heated cavity at Rayleigh number Ra , the vertical walls being isothermal and the horizontal walls insulating, see [20, 13]. The fluid is air, with Prandtl number $Pr = 0.71$, initially at rest at the reference temperature $\mathcal{T}_0 = 300\text{ K}$ and atmospheric pressure $p_0 = 101325\text{ Pa}$. The vertical wall temperatures are respectively maintained at $\mathcal{T}_h = \mathcal{T}_0 + \delta\mathcal{T}/2$ and $\mathcal{T}_c = \mathcal{T}_0 - \delta\mathcal{T}/2$. Then, the convection flow is driven by the gravity force $\mathbf{f} = \rho \mathbf{g}$ at a low Mach number regime with $Ma \approx 10^{-3}$. When the characteristic temperature difference $\delta\mathcal{T}$ is less than a few degrees, the Boussinesq approximation is valid, the flow remains stationary up to $Ra = 2 \cdot 10^8$, and we refer to [20] for reference solutions computed with pseudo-spectral methods. The Nusselt number Nu , representing the ratio between the total heat transfer and the diffusive heat transfer, is very sensitive to the quality of the numerical solution since it incorporates both the dynamics and thermal effects. We use a Richardson extrapolation to estimate the reference Nusselt number Nu_{ref} from [20] or Nu_∞ from the present computations, when the number of mesh points M per space direction tends to infinity. The comparison given in Table 1 for $\delta\mathcal{T} = 1.06\text{ K}$ and $Ra = 10^5$ shows a perfect agreement until the fifth digit between the three methods which have all a second-order convergence of the Nusselt number with the mesh step $h = 1/M$. Let us notice that the present computations does not use the Boussinesq approximation, but suppose that the fluid is dilatable as a perfect gas.

Mesh	8	16	32	64	128	256	512	1024	Nu_∞	Order	Nu_{ref}
UAL	3.3543	4.1332	4.4134	4.4937	4.5146	4.5198	4.5212	4.5215	4.5216	2	4.5216
SIP	3.3543	4.1332	4.4134	4.4937	4.5146	4.5198	4.5212	4.5215	4.5216	2	4.5216
VPP	3.3543	4.1332	4.4134	4.4937	4.5146	4.5198	4.5212	4.5215	4.5216	2	4.5216

Table 1: Natural convection at $Ra = 10^5$ - Comparison of the (UAL), (SIP) and (VPP) methods on uniform MAC meshes of size M .

Moreover, we study the convergence properties of the velocity correction step (5) for this sharp test case. Again, we get the convergence of the velocity divergence as $O(\varepsilon \delta t)$: more precisely, we obtain: $\|\nabla \cdot \mathbf{v}\|_{L^2(\Omega)} \approx 4.3 \cdot 10^{-4} \varepsilon \delta t$; see also Figure 2 (right). We can reach the machine precision of 10^{-15} for double precision floating point computations. Besides, the solution of the *penalty-correction step* (5) proves to be all the cheaper as $\eta = \varepsilon/\delta t$ tends to zero, as expected from Theorem 3.1. Indeed, we have observed that for $\eta = \varepsilon/\delta t \leq 10^{-6}$, only one or two iterations of the ILU(0)-BiCGStab2 preconditioned Krylov solver are sufficient to get an accurate approximation up to machine precision of the operator $C_0 = -I_0$ in Theorem 3.1, and that independently of the mesh size h as shown in Figure 3.

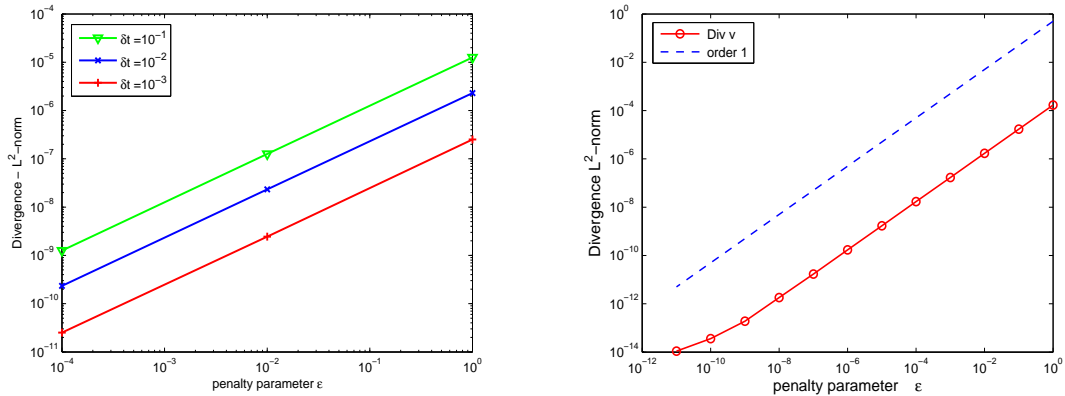


Figure 2: (VPP) $_\varepsilon$ method - LEFT: velocity divergence versus penalty ε for the Green-Taylor vortex at $Re = 100$, $t = 10$ - $h = 1/512$, $\|res\|_2 \leq 10^{-10}$. RIGHT: divergence L^2 -norm vanishing as $O(\varepsilon)$ for the thermal convection at $Ra = 10^5$, $t = 1$ with $\delta t = 1$, $h = 1/256$, $\|res\|_2 \leq 10^{-16}$.

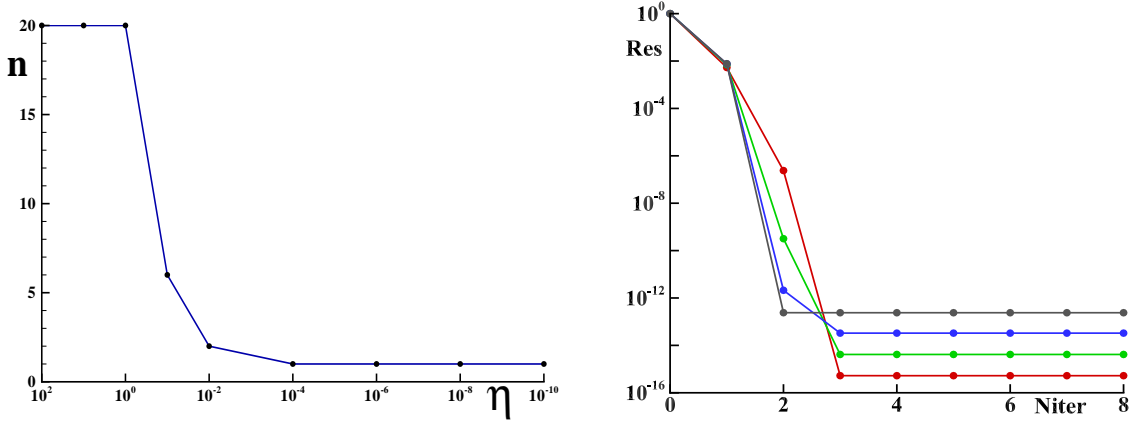


Figure 3: Convergence of ILU(0)-BiCGstab2 for (VPP) correction step – LEFT: number of iterations versus $\eta = \varepsilon/\delta t$ for natural convection at $Ra = 10^5$ with $t = 2\delta t$, $\delta t = 1$, $h = 1/256$, $\|res\|_2 \leq 10^{-6}$. RIGHT: normalized residual (by initial residual) versus number of iterations for different mesh sizes 32×32 (red), 128×128 (green), 512×512 (blue) and 2048×2048 (black) with $\eta = 10^{-14}$.

4.3. Multiphase flows: dispersed two-phase bubble dynamics

The (VPP _{ε}) method is now numerically validated for multiphase incompressible flows by performing with the three methods (UAL), (SIP) and (VPP), the benchmark problem studied in [16] for 2-D bubble dynamics. In that problem, we compute the first test case which considers an initial circular bubble of diameter 0.05 m with density and viscosity ratios equal to 10 which undergoes moderate shape deformation. The results from all codes in [16] agree here very well allowing for target reference values to be established, whereas they are very different for the second test case with larger density or viscosity jumps. In this case, the bubble is driven up by the external gravity force $\mathbf{f} = \rho \mathbf{g}$, whereas the surface tension effect on the interface Σ between the two fluid phases is taken into account through the following force balance at the interface Σ :

$$[[\mathbf{v}]]_{\Sigma} = 0 \quad \text{and} \quad [[(-p\mathbf{I} + \mu(\nabla\mathbf{v} + (\nabla\mathbf{v})^T)) \cdot \mathbf{n}]]_{\Sigma} = \sigma \kappa \mathbf{n}_{\Sigma}, \quad \text{or} \quad \mathbf{f}_{st} = \sigma \kappa \mathbf{n}_{\Sigma} \delta_{\Sigma}$$

where $\sigma = 24.5$ is the surface tension coefficient, κ the local curvature of the interface, \mathbf{n}_{Σ} the outward unit normal to the interface and δ_{Σ} the Dirac measure supported by the interface Σ ; see the well-posedness of fluid flow problems with such jump embedded conditions in [2]. The solution of the phase transport (3) is carried out by the so-called *VOF-PLIC* method, *i.e.* the famous *VOF* method using a piecewise linear interface construction proposed in [24] to precisely reconstruct the sharp interface Σ at the isoline $\varphi = 0.5$, with $\varphi^0 = 0$ in Ω_1 and $\varphi^0 = 1$ in Ω_2 ; see [22, 23]. As usual, the stability of the explicit transport scheme (8) needs to satisfy a *CFL* condition. This method has been precisely validated in several works for multiphase flows by comparison with other interface front-tracking methods, *e.g.* [21]. The sharp interface tracking for two immiscible phases is then achieved by calculating at each time step the density and viscosity fields from the phase field $\varphi \in [0, 1]$ as follows, H denoting the Heaviside function:

$$\rho(\varphi) = \rho_1 (1 - H(\varphi - 0.5)) + \rho_2 H(\varphi - 0.5), \quad \mu(\varphi) = \mu_1 (1 - H(\varphi - 0.5)) + \mu_2 H(\varphi - 0.5)$$

The results of the three methods (UAL), (SIP) and (VPP) after 420 time iterations are presented in Figure 4 by superposing the different fields to get a more precise comparison. In particular, the discontinuity of the pressure field at the interface Σ induced by the normal stress jump is well resolved as shown in Figure 4 (left). Here also, we observe an excellent agreement both between the three methods and the reference solution in [16]. Indeed, a zoom comparison for the isoline $\varphi = 0.5$ of the phase function at the interface Σ shows a difference of order $O(h/50)$ with respect to the mesh step h between the three methods. However, the (VPP) method runs faster.

4.4. A test case for fluid-structure interaction problems

To evaluate the robustness of the (VPP _{ε}) method with respect to large density or viscosity ratios, we finally compute the motion of an heavy solid ball which freely falls vertically in air with the gravity force $\mathbf{f} = \rho_s \mathbf{g}$. The rigid behaviour of the body is obtained by letting the viscosity μ_s tend to infinity inside the ball in order to penalize

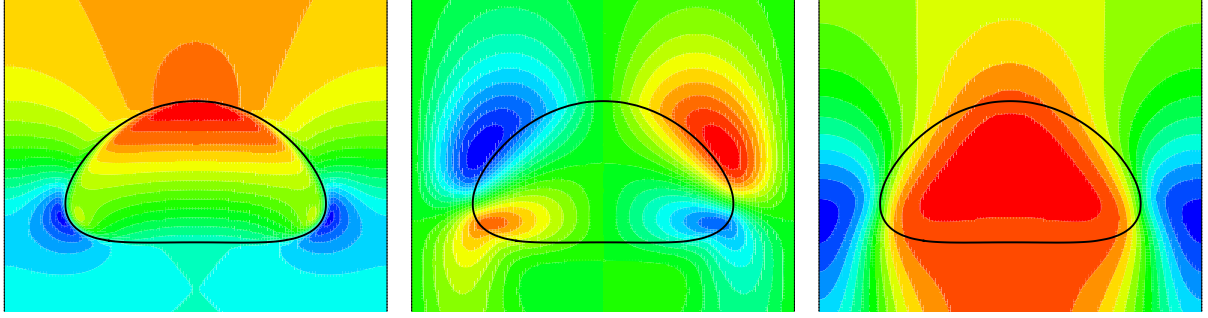


Figure 4: Benchmark for 2-D bubble dynamics with (VPP_ε) method, $\varepsilon = 10^{-8}$: motion of a circular bubble with surface tension at time $t = 3$ and $Re = 35$ - bubble initial diameter $\varnothing = 0.05$, $\rho_1/\rho_2 = 1000/100 = 10$, $\mu_1/\mu_2 = 10/1 = 10$, domain 0.1×0.2 , mesh size 128×256 , $\delta t = 0.007143$, circular bubble initially with no motion at height $y = 0.05$. LEFT: isobars and isoline $\varphi = 0.5$ of the phase function at interface. CENTER: horizontal velocity field. RIGHT: superposition of isoline $\varphi = 0.5$ at interface for (UAL), (SIP), (VPP) and vertical velocity field (in absolute referential).

the tensor of deformation rate $\mathbf{d}(\mathbf{v})$. This fictitious domain method using a volume penalty was early proposed in [4] to design a numerical wind-tunnel, and then numerically validated in several works, see [23], and also analysed theoretically in [1, 3] where optimal global error estimates are proved for the H^1 penalty method. Moreover, this fictitious domain method allows us to easily compute the forces applied on the obstacle as proposed in [11] and numerically validated in [19]; the error estimate being proved in [1] when the nonlinear convection term is neglected inside the solid obstacle.

The results obtained with the (VPP_ε) method are presented in Figure 5 at time $t = 0.15$ s after 750 time iterations when the ball nearly reaches the theoretical velocity: $V_b = g t = 1.4715$ m/s obtained by neglecting the drag force which is very small in air. In this case, the density ratio equals 10^6 and the viscosity ratio is 10^{17} . The computation shows that the strain rate tensor inside the ball Ω_s vanishes as $\|\mathbf{d}(\mathbf{v})\|_{L^2(\Omega_s)} = O(\mu_f/\mu_s)$ in agreement with the error estimate for the H^1 volume penalty in [3], *i.e.* here of the order of the machine precision. Hence, the (VPP_ε) method efficiently ensures both the rigidity of the solid body and a velocity divergence vanishing as $O(\varepsilon \delta t)$ [5, 6], whereas it avoids the locking effect observed with other methods, *e.g.* [23].

The (SIP) method crashes after a few time iterations. The (UAL) method is still able to compute the flow with a much larger velocity divergence and computational time than with the (VPP_ε) method. Hence, a key feature of the proposed (VPP_ε) method is that the solution to the linear system associated with the vector penalty-projection step can be very fast and cheap whatever the spatial mesh size because of the adapted form of the right-hand side. Indeed, the (VPP_ε) method really takes advantage of the splitting of augmented Lagrangian systems within a prediction and an adapted correction steps as proposed and analysed in [7].

5. Conclusion and perspectives

We have presented and numerically validated a new vector penalty-projection method (VPP_ε) for the solution of non-homogeneous or multiphase incompressible flows. This method proves to be really promising since it is fast, cheap, and very robust whatever the density or viscosity jumps. Indeed, our method can efficiently and accurately compute some severe test cases, whereas other famous methods fail.

References

- [1] PH. ANGOT, Analysis of singular perturbations on the Brinkman problem for fictitious domain models of viscous flows, *Math. Meth. in the Appl. Sci. (M2AS)* **22**(16), 1395-1412, 1999.
- [2] PH. ANGOT, A fictitious domain model for the Stokes/Brinkman problem with jump embedded boundary conditions, *C. R. Math. Acad. Sci. Paris, Ser. I* **348**(11-12), 697-702, 2010.
- [3] PH. ANGOT, C.-H. BRUNEAU AND P. FABRIE, A penalization method to take into account obstacles in incompressible viscous flows, *Numerische Mathematik* **81**(4), 497-520, 1999.
- [4] PH. ANGOT AND J.P. CALTAGIRONE, New graphical and computational architecture concept for numerical simulation on supercomputers, *Proceedings 2nd World Congress on Computational Mechanics, Stuttgart, Vol. 1*, pp. 973-976, Aug. 1990.
- [5] PH. ANGOT, J.-P. CALTAGIRONE AND P. FABRIE, Vector penalty-projection methods for the solution of unsteady incompressible flows, in *Finite Volumes for Complex Applications V - Problems & Perspectives*, R. Eymard and J.-M. Hérard (Eds), pp. 169-176, ISTE Ltd and J. Wiley & Sons, 2008.

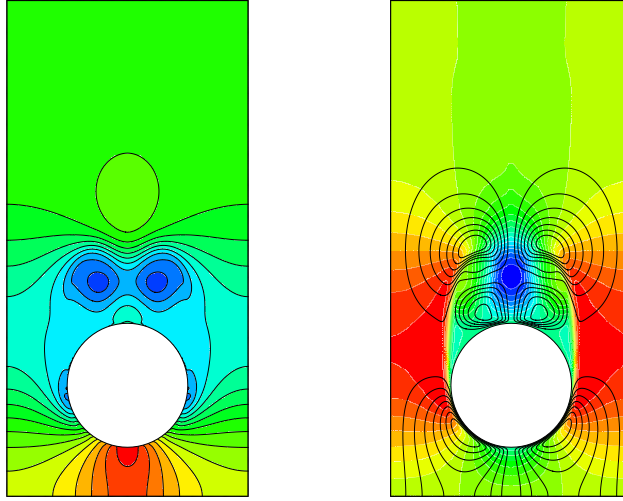


Figure 5: ACF11-ball with (VPP_ε) method, $\varepsilon = 10^{-6}$: free fall of a heavy solid ball in air at time $t = 0.15$ and $\text{Re} = 7358$ - Cylinder diameter $\varnothing = 0.05$, $\rho_s = 10^6$, $\rho_f = 1$, $\mu_s = 10^{12}$, $\mu_f = 10^{-5}$, domain 0.1×0.2 , mesh size 256×512 , $\delta t = 0.0002$, cylinder initially with no motion at height $y = 0.15$. LEFT: isobars and isoline $\varphi = 0.5$ of the phase function at interface. RIGHT: vertical velocity field and horizontal velocity isolines.

- [6] PH. ANGOT, J.-P. CALTAGIRONE AND P. FABRIE, A spectacular vector penalty-projection method for Darcy and Navier-Stokes problems, in *Finite Volumes for Complex Applications VI - Problems & Perspectives*, J. Fořt et al. (Eds), Springer Proceedings in Mathematics **4**, Vol. 1, pp. 39-47, Springer-Verlag (Berlin), 2011.
- [7] PH. ANGOT, J.-P. CALTAGIRONE AND P. FABRIE, A new fast method to compute saddle-points in constrained optimization and applications, *Applied Mathematics Letters* **25**(3), 245-251, 2012.
- [8] PH. ANGOT AND P. FABRIE, Convergence results for the vector penalty-projection and two-step artificial compressibility methods, *Discrete and Continuous Dynamical Systems, Serie B*, 2012 (to appear).
- [9] PH. ANGOT, M. JOBELIN AND J.-C. LATCHÉ, Error analysis of the penalty-projection method for the time-dependent Stokes equations, *Int. J. on Finite Volumes (IJFV)* **6**(1), 1-26, 2009.
- [10] J. BLAIR PEROT, Discrete conservation properties of unstructured mesh schemes, *Annu. Rev. Fluid Mech.* **43**, 299-318, 2011.
- [11] J.-P. CALTAGIRONE, On the fluid-porous interaction; application to the calculation of efforts exerted on an obstacle by a viscous fluid, *C. R. Acad. Sci. Paris, Serie IIB* **318**, 571-577, 1994.
- [12] J.-P. CALTAGIRONE AND J. BREIL, Sur une méthode de projection vectorielle pour la résolution des équations de Navier-Stokes, *C. R. Acad. Sci. Paris, Serie IIB* **327**, 1179-1184, 1999.
- [13] J.-P. CALTAGIRONE, K. KHADRA AND PH. ANGOT, On a local multigrid mesh refinement method for solving Navier-Stokes Equations, *C. R. Acad. Sci. Paris, Serie IIB* **320**(6), 295-302, 1995.
- [14] C. FÉVRIÈRE, J. LAMINIE, P. POULLET AND PH. ANGOT, On the penalty-projection method for the Navier-Stokes equations with the MAC mesh, *J. Comput. Appl. Math. (JCAM)* **226**(2), 228-245, 2009.
- [15] J.-L. GUERMOND, P.D. MINEV AND J. SHEN, An overview of projection methods for incompressible flows, *Comput. Meth. Appl. Mech. Engrg.* **195**, 6011-6045, 2006.
- [16] S. HYSING, S. TUREK, D. KUZMIN, N. PAROLINI, E. BURMAN, S. GANESAN AND L. TOBISKA, Quantitative benchmark computations of two-dimensional bubble dynamics, *Int. J. Numer. Meth. Fluids*, **60**, 1259-1288, 2009.
- [17] M. JOBELIN, C. LAPUERTA, J.-C. LATCHÉ, PH. ANGOT AND B. PIAR, A finite element penalty-projection method for incompressible flows, *J. Comput. Phys.* **217**(2), 502-518, 2006.
- [18] M. JOBELIN, B. PIAR, PH. ANGOT AND J.-C. LATCHÉ, Une méthode de pénalité-projection pour les écoulements dilatables, *European J. of Computational Mechanics* **17**(4), 453-480, 2008.
- [19] K. KHADRA, PH. ANGOT, S. PARNEIX AND J.-P. CALTAGIRONE, Fictitious domain approach for numerical modelling of Navier-Stokes equations, *Int. J. Numer. Meth. in Fluids*, **34**(8), 651-684, 2000.
- [20] P. LE QUÉRE, Accurate solutions to the square thermally driven cavity at high Rayleigh numbers, *Computers and Fluids* **20**(1), 29-41, 1991.
- [21] G. PIANET, S. VINCENT, J. LEBOI, J.-P. CALTAGIRONE AND M. ANDERHUBER, Simulating compressible gas bubbles with a smooth volume tracking 1-Fluid method, *Int. J. Multiphase Flow*, **36**, 273-283, 2010.
- [22] A. SARTHOU, S. VINCENT, J.-P. CALTAGIRONE AND PH. ANGOT, Eulerian-Lagrangian grid coupling and penalty methods for the simulation of multiphase flows interacting with complex objects, *Int. J. Numer. Meth. in Fluids* **56**(8), 1093-1099, 2008.
- [23] S. VINCENT, A. SARTHOU, J.-P. CALTAGIRONE, F. SONILHAC, P. FÉVRIER, C. MIGNOT AND G. PIANET, Augmented Lagrangian and penalty methods for the simulation of two-phase flows interacting with moving solids. Application to hydroplaning flows interacting with real tire tread patterns, *J. Comput. Phys.* **230**, 956-983, 2011.
- [24] D.L. YOUNGS, Time-dependent multimaterial flow with large fluid distortion, in *Numerical Methods for Fluid Dynamics*, K.W. Morton, M.J. Baines (Eds.), Academic Press (New York), 1982.